

## Electrochemical Behaviour of Doxorubicin Encapsulated in Apoferritin

Katerina Tmejova<sup>1,2</sup>, David Hynek<sup>1,2</sup>, Pavel Kopel<sup>1,2</sup>, Simona Dostalova<sup>1</sup>, Kristyna Smerkova<sup>1</sup>, Maja Stanisavljevic<sup>1</sup>, Hoi Viet Nguyen<sup>1</sup>, Lukas Nejd<sup>1</sup>, Marketa Vaculovicova<sup>1,2</sup>, Sona Krizkova<sup>1,2</sup>, Rene Kizek<sup>1,2</sup>, Vojtech Adam<sup>1,2\*</sup>

<sup>1</sup> Department of Chemistry and Biochemistry, Faculty of Agronomy, Mendel University in Brno, Zemedelska 1, CZ-613 00 Brno, Czech Republic, European Union

<sup>2</sup> Central European Institute of Technology, Brno University of Technology, Technicka 3058/10, CZ-616 00 Brno, Czech Republic, European Union

\*E-mail: [vojtech.adam@mendelu.cz](mailto:vojtech.adam@mendelu.cz)

Received: 14 April 2013 / Accepted: 22 August 2013 / Published: 20 October 2013

---

A voltammetric detection of doxorubicin and encapsulated doxorubicin in apoferritin structure at a carbon paste electrode is the main aim of this study. The samples were measured by differential pulse voltammetry in phosphate buffer (pH 5.5). Complex apoferritin-doxorubicin can be formed by “opening”/“closing” due to changing of pH value. The pH value of electrolyte was decreased and sample of encapsulated doxorubicin was done by adding of hydrochloric acid. We optimized the experimental conditions as time of accumulation and deposition potential to obtain detection limit for encapsulated doxorubicin of 1.0 µg/ml of doxorubicin.

---

**Keywords:** electrochemical detection; apoferritin; doxorubicin; carbon paste electrode; spectrophotometry; capillary electrophoresis; nanomedicine

### 1. INTRODUCTION

Doxorubicin ((8S,10S)-10-(4-amino-5-hydroxy-6-methyl-tetrahydro-2H-pyran-2-yloxy)-6,8,11-trihydroxy-8-(2-hydroxyacetyl)-1-methoxy-7,8,9,10-tetrahydrotetracene-5,12-dione) called also as adriamycin is an anthracycline antibiotic (inset in Fig. 1A). It is commonly used in the treatment of a wide range of malignancies. The exact mechanism of action of doxorubicin is complex and still somewhat unclear. The current accepted mechanisms are intercalation into DNA and topoisomerase II inhibition [1-6]. However, its toxicity and association with the development as substantial cardiotoxicity decreases wider using of the drug in therapy [1,7-10]. Generating of reactive oxygen

species causing lipoperoxidation that cause damaging of cell membranes, apoptotic changes via interaction with iron ions and activation of NF $\kappa$ B belongs to the other important effect of doxorubicin *in vivo* [1,3,11]. Thus, the main accent is to reduce the toxicity and find some transporter of this cytostatic to the cancer cells [12-14]. Successful process how to reach both points is encapsulation of anticancer drug into some transporter [15-17]. Numerous transporter systems like protein-based carriers [18], liposomes [19] and antibodies [20] have been suggested. It seems that intracellular protein apoferritin could be considered as a promising compound for transport [21-23], because contains a cage with internal and external diameters of 8 and 12 nm, respectively [24]. Apoferritin-binding sites [25] and endocytosis of apoferritin [26] have been identified in neoplastic cells and apoferritin may improve the drug selectivity for cell surfaces that express ferritin receptors. Due to the fact that it is possible to form complex apoferritin-doxorubicin by “opening” and “closing”, apoferritin receptors could be suitable candidate for anticancer drug delivering [27]. Encapsulated doxorubicin can be free by pH changing to the acidic and doxorubicin can attack cancer cells [28,29].

The electrochemical detection of doxorubicin (and other related drugs) is possible due to electroactivity of these molecules [30-43]. Doxorubicin is a complex molecule, where quinone and hydroquinone groups are electroactive and can be used to identify electrochemical reduction and/or oxidation of the drug [44,45]. Studies have been carried with mercury, carbon and other types of modified electrodes [46-49]. Polarographic behaviour of doxorubicin has been investigated by several authors with good sensitivity [31,50-53]. Carbon paste electrodes are superior to other solid electrodes in having a low residual current a noise [54] and due to the fact that their preparation is easy. These electrodes can be used for both cathodic and anodic based assays [55]. Basic electrochemical behaviour of doxorubicin at carbon paste electrode (CPE) has been investigated by several authors [56-60]. Application of carbon nanotubes (CNT) modified electrode for electrochemical detection of doxorubicin was also suggested [59,61]. The interaction between the CNT and the anthracycline could enhance the electron transfer, which increased the detection sensitivity and lowered the detection limit [62]. It can be predicted that many more analogues could be monitored on such a platform with high sensitivity [63].

The main aim of this study was encapsulating of doxorubicin into apoferritin structure. It was achieved by reassembly route. At low pH (addition of HCl) apoferritin structure opens and the structure is reconstituted again after addition of base. In the presence of doxorubicin in solution some amount of doxorubicin is caught inside the cavity. This encapsulating/opening was detected using differential pulse voltammetry at expanded carbon paste electrode.

## 2. EXPERIMENTAL PART

### 2.1 Chemicals and material

Doxorubicin drug solution (2 mg/ml) was obtained from Teva Pharmaceuticals CR (Czech Republic). Other chemicals used in this study were purchased from Sigma-Aldrich (USA) in ACS

purity unless stated otherwise. Pipetting was performed by certified pipettes (Eppendorf, Germany). The deionised water was prepared using reverse osmosis equipment Aqual 25 (Czech Republic). The deionised water was further purified by using apparatus MiliQ Direct QUV equipped with the UV lamp. The resistance was 18 M $\Omega$ . The pH was measured using pH meter WTW inoLab (Weilheim, Germany).

### 2.2 Preparation of encapsulated doxorubicin in apoferritin

20  $\mu$ l of apoferritin solution (50 mg/ml, equine spleen, Sigma-Aldrich) was diluted with 200  $\mu$ l of ACS water. Doxorubicin (100  $\mu$ l, 2 mg/ml) was added and mixture was shaken. 1 M HCl (0.5  $\mu$ l) was added and turbidity was observed. 15 min later, 1 M NaOH (0.5  $\mu$ l) was added and turbidity disappeared. Solution was subsequently 2 h shaken on Vortex Genie2 (Scientific Industries, USA). Dialyses for 24 h were realized on membrane filter (0.025  $\mu$ m VSWP, Millipore) against 2 l of water. The obtained solution was diluted with ACS water to final volume of 1 ml [64].

### 2.3 Preparation of biotinylated apoferritin filled with doxorubicin

Biotinamidohexanoyl-6-aminohexanoic acid 100  $\mu$ l (1 mg/ml) was added to the solution of apoferritin doxorubicin complex prepared according to protocol mentioned in Section 2.2. The mixture was shaken for 2 h on Vortex Genie2 and dialysis was accomplished as previously.

### 2.4 Isolation of doxorubicin encapsulated in biotinylated apoferritin using streptavidin magnetic beads

Dynabeads M-270 Streptavidin (Life Technologies, cat. 65305, USA) were resuspended and 100  $\mu$ l beads were pipetted to the tube. The tube was placed to magnetic holder and kept there for 2 min. The supernatant was carefully sucked out. The tube was removed from holder and 100  $\mu$ l phosphate buffered saline (PBS, pH 7.4) was added to the solution for washing. The whole solution was resuspended. Washing was repeated 3 times. In the end, supernatant was sucked out and 100  $\mu$ l of sample (biotinylated apoferritin) was added. Solution was incubated at room temperature on rotator (60 rpm, 90 °C) for 30 min, vibration was turned off. Tube was put to magnetic holder for 3 min and supernatant was poured out. Particles were 3 or 4 times rinsed with 100  $\mu$ l PBS (pH 7.4), after that they were resuspended in 100  $\mu$ l PBS (pH 7.4).

### 2.5 Carbon paste electrode

The expanded carbon used in this study was obtained from Brno University of Technology, Brno, Czech Republic. The expanded carbon was prepared from natural graphite in the range 1:1 with

sulphuric acid. This mixture was oxidized by hydrogen peroxide (50%) for strong reaction in stainless steel reactor. After this reaction graphite material was placed to the muffle/vacuum oven and left to expand at 850 °C. Expanding took 30 s. Natural graphite increases its volume few times during this reaction. Conductivity of this material is dependent on flakes size and is proportionally to flakes size [65]. The paste was prepared by mixing 0.1 g of expanded powder and 200 µl mineral oil in a mortar and then well homogenized. After homogenization the electrode body was manually filled and pressed. The surface of electrode was renewed by polishing on the filter paper before each measurement. One set of measurement (calibration) was done with one prepared expanded carbon paste.

### 2.6 Electrochemical analysis

Electrochemical measurements were performed using a CH Instruments Electrochemical Workstation (CH Instruments, USA), using glass cell with three electrodes. Expanded carbon paste was used as a working electrode. Ag/AgCl/3M KCl was reference electrode (Metrohm, Switzerland) and counter electrode was platinum (Metrohm). The differential pulse voltammetry parameters were as follows: initial potential -1.0 V, end potential 0 V, pulse width 0.2 s, pulse period 0.5 s, deposition potential -1.0 V and time of accumulation 120 s (for doxorubicin) and 0 s (for encapsulated doxorubicin). All experiments were carried out at room temperature. 0.1 M potassium phosphate buffer (pH 5.5 and lower) was used as the electrolyte. Measuring solution consisted from 10 µl of sample and 1990 µl of phosphate buffer for doxorubicin and from 100 µl of sample and 1900 µl of phosphate buffer for encapsulated doxorubicin. CHI 440A software was applied for data treatment [4].

### 2.7 Spectrophotometry

Absorbance spectrum of doxorubicin was measured at spectrophotometer SPECORD 210 (Analytik Jena, Germany) within the range from 200 to 800 nm. The quartz cuvettes with optical path 1 cm (Hellma Essex, UK) were used for measurement. Cell area was tempered to 20 °C by thermostat Julabo (Labortechnik, Wasserburg, Germany). Water was used as the baseline reference.

### 2.8 Capillary electrophoresis

Electrophoretic measurement was done using capillary electrophoresis system (Agilent Technology, Capillary electrophoresis 7100) with absorbance detection at wavelength 200 nm. Uncoated fused silica capillary ( $l_{\text{tot}} = 48.5$  cm,  $l_{\text{eff}} = 40$  cm and ID = 75 µm) was used. 20 mM borate (pH 9.2) was used as background electrolyte. Separation was carried out at 20 kV with hydrodynamic injection for 10 sec by 3.4 kPa. Sample of doxorubicin was diluted 1:1 or (1:100) with buffer with final concentration of 1 mg/ml (0.02 mg/ml).

### 2.9 Gel electrophoresis

The verification of doxorubicin and apoferritin was done by gel electrophoresis on 6% non-denaturing native PAGE (60 mM glycine, 7 mM acetic acid pH 4) loading buffer (50% glycerol), 10 mA, 90 min. Bands were visualized by Coomassie-blue.

### 2.10 Mathematical treatment of data and estimation of detection limits

Data were processed using MICROSOFT EXCEL® (USA) and STATISTICA.CZ Version 8.0 (Czech Republic). Results are expressed as mean  $\pm$  standard deviation (S.D.) unless noted otherwise (EXCEL®). The detection limits (3 signal/noise, S/N) were calculated, whereas N was expressed as standard deviation of noise determined in the signal domain unless stated otherwise [66].

## 3. RESULTS AND DISCUSSION

Doxorubicin as a widely used anticancer drug has great side effects including cardiotoxicity. Elimination of these ones is possible due to encapsulation of doxorubicin to the apoferritin structure. This model was achieved simply by changing the proton concentration of the external solution. It is the easier way than by the modification of drug or carrier molecules. Application of electrochemical analysis using carbon paste electrodes, as popular electrodes in the field of electroanalytical methods [67-73], for description of this model is the main aim of this study.

### 3.1 Doxorubicin detection on the carbon paste electrode

For the electrochemical detection of doxorubicin expanded carbon was applied. This electrode material was chosen with regard to our previous works [64,74], in which we investigated various carbon powders used for carbon paste electrode preparation. Doxorubicin was measured at CPE by differential pulse voltammetry. The obtained DP voltammograms showed two characteristic peaks (D1 peak at -0.55 V and D2 peak at -0.68 V, Fig. 1A). The first optimized parameter was time of accumulation of sample on the electrode surface within the interval from 0 to 240 s (Fig. 1A). To study the effect of this parameter, heights of both peaks were determined. It clearly follows from the obtained results that no changes occurred. Therefore time of accumulation 0 s was selected as the optimum for the following experiments.

Measurements of doxorubicin were carried out in the presence of potassium phosphate buffer. Thus, the influence of buffer pH was another parameter, which was optimized. pH of the electrolyte was changed within the range from 1 to 5.5. In the pH range from 1.0 to 3.5, no changes of peak height were detected (Fig. 1B, the main y axis). From pH 4.0 to 5.5 the increase height of both doxorubicin

signals was observed. The height of peak D1 increased more steeply compared to D2 peak and at pH 5.5 this peak became higher than D2. For the following experiments, pH of phosphate buffer 5.5 was selected. Dependences of potential changes of peaks D1 and D2 increased with the increasing pH (Fig. 1B, secondary y axis). The changes in peak heights are shown in insets in Fig. 1B.

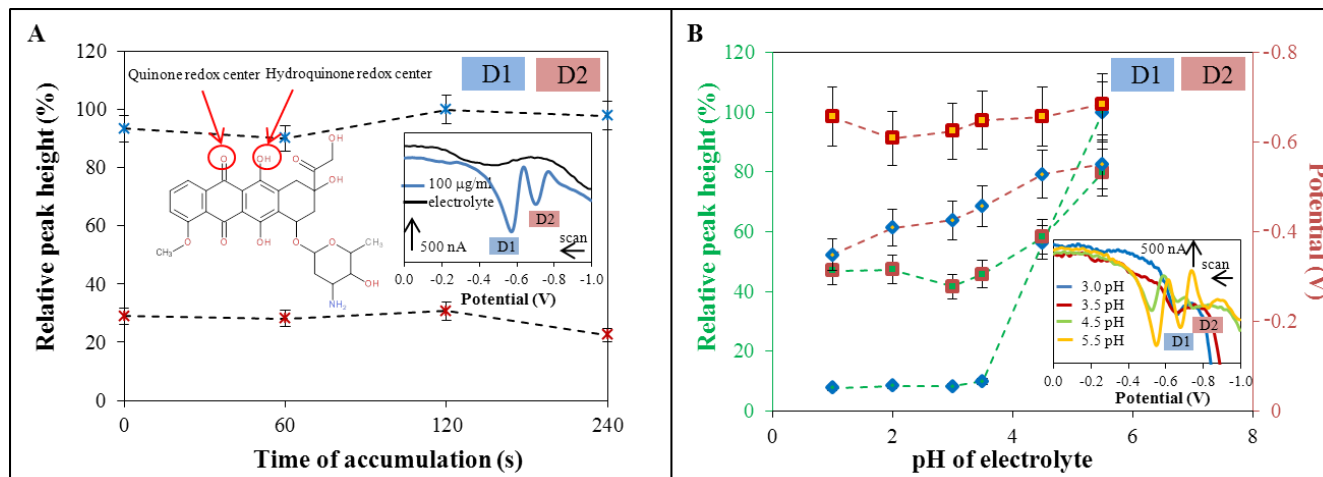


**Figure 1.** Characterisation of electrochemical signal for doxorubicin. (A) Dependence of relative peak height on accumulation time for 100 µg/ml doxorubicin; in the left inset: scheme of doxorubicin with two outline position (quinone redox and hydroquinone redox centre). Inserted voltammogram of doxorubicin (100 µg/ml) has two characteristic peaks D1 at the potential -0.55 V and at the potential D2 -0.68 V, electrolyte has pH 5.5. (B) Dependence of relative peak height (green axis) on electrolyte pH, peak at -0.55 V (♦) and at -0.68 V (■), change of peak position (orange axis) on electrolyte pH, peak at -0.55 V (◆) and at -0.68 V (■), doxorubicin concentration 100 µg/ml. Inserted voltammogram shows changing of height or disappearance of some peak due to pH of electrolyte. This effect is demonstrated for pH 3.0, 3.5, 4.5 and 5.5. All experiments were measured by DPV with the following parameters: initial potential -1.0 V, end potential 0 V, amplitude 0.05 V, pulse width 0.2 s, pulse period 0.5 s, deposition potential -1.0 V and time of accumulation 120 s. Phosphate buffer with different pH (0.1 M) was used as a supporting electrolyte.

**Table 1.** Analytical parameters of electrochemical determination of doxorubicin based on D1 peak detected at - -0.55 V.

Substance	Regression equation	Linear dynamic range (µM)	Linear dynamic range (µg/ml)	R2 <sup>1</sup>	LOD <sup>2</sup> (µM)	LOD (µg/ml)	LOQ <sup>3</sup> (µM)	LOQ (µg/ml)	RSD <sup>4</sup> (%)
doxorubicin	y = 5.407x+29.21	1.44 – 184	0.78 – 100	0.988	10	6	40	20	19

- 1...regression coefficients
- 2...limit of detection (3 S/N)
- 3... limit of quantification (10 S/N)
- 4...relative standard deviation

**Table 2.** Analytical parameters of electrochemical determination of doxorubicin based on D2 peak detected at -0.68V.

Substance	Regression equation	Linear dynamic range ( $\mu\text{M}$ )	Linear dynamic range ( $\mu\text{g/ml}$ )	$R^2$ <sup>1</sup>	LOD <sup>2</sup> ( $\mu\text{M}$ )	LOD ( $\mu\text{g/ml}$ )	LOQ <sup>3</sup> ( $\mu\text{M}$ )	LOQ ( $\mu\text{g/ml}$ )	RSD <sup>4</sup> (%)
doxorubicin	$y = 2.999x + 135.66$	2.87 – 184	1.56 – 100	0.961	60	30	200	100	20

- 1...regression coefficients
- 2...limit of detection (3 S/N)
- 3...limit of quantification (10 S/N)
- 4...relative standard deviation

The last step of optimization process was determination of calibration under the optimal conditions (Fig. 2A). It is shown that the both concentration dependences had linear characteristic and D1 peak was found linear within doxorubicin concentration from 0.78 to 100  $\mu\text{g/ml}$  and D2 peak within doxorubicin concentration from 1.56 to 100  $\mu\text{g/ml}$ . For D1 peak, the equation was  $y = 5.407 x + 29.214$ ,  $R^2 = 0.988$ ,  $n = 4$ , R.S.D. = 19 (Table 1) and for D2 peak  $y = 2.999 x + 135.66$ ,  $R^2 = 0.961$ ,  $n = 4$ , R.S.D. = 20 (Table 2).

### 3.2 UV – VIS spectroscopy and capillary electrophoresis of doxorubicin

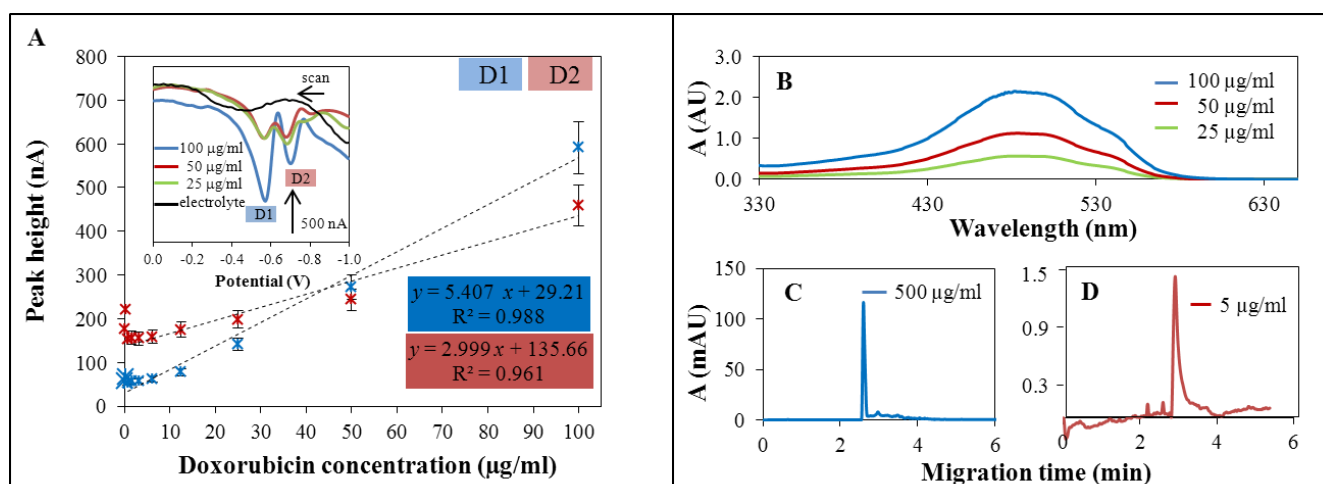


**Figure 2.** Characterisation of doxorubicin. (A) Calibration curves of doxorubicin in phosphate buffer, pH 5.5. Dependences were measured for two peaks (blue dots – peak around -0.55 V, red dots – around -0.68 V). The final value was done from 4 replicates. Inset: Voltammogram shows real data for the three highest concentrations (blue line – 100  $\mu\text{g/ml}$ , red line - 50  $\mu\text{g/ml}$ ). DPV parameters were as it follows: Initial potential -1.0 V, end potential 0 V, amplitude 0.05 V, pulse width 0.2 s, pulse period 0.5 s, deposition potential -1.0 V and time of accumulation 120 s. Phosphate buffer (0.1 M, pH 5.5) was used as a supporting electrolyte. (B) The spectrum of doxorubicin (blue line – 100  $\mu\text{g/ml}$ , red – 50  $\mu\text{g/ml}$  and green line – mg25  $\mu\text{g/ml}$ ). (C, D) The pictures show electropherograms of doxorubicin in 20 mM borate buffer (pH 9.2); Separation conditions: capillary:  $l_{\text{eff}}/l_{\text{tot}} = 40/48.5$  cm, id = 75 mm; injection: 10 s, 3.4 kPa; voltage: 20 kV; absorbance 200 nm.

For description of doxorubicin absorbance spectrum of doxorubicin 25 and 50, 100  $\mu\text{g/ml}$  was measured in ACS water (Fig. 2B). It was found that spectrum had maximum at 474 nm and two shoulders at 498 and 540 nm, which is in accordance with Yousefpour et al. [75]. The migration time of doxorubicin of 5 and 500  $\mu\text{g/ml}$  was measured by capillary electrophoresis. The migration time was  $\sim 2.8$  min (Figs. 2C and D). The biophysical characteristics of the doxorubicin enabled us to direct other experiments.

### 3.3 Encapsulating of doxorubicin into apoferritin structure

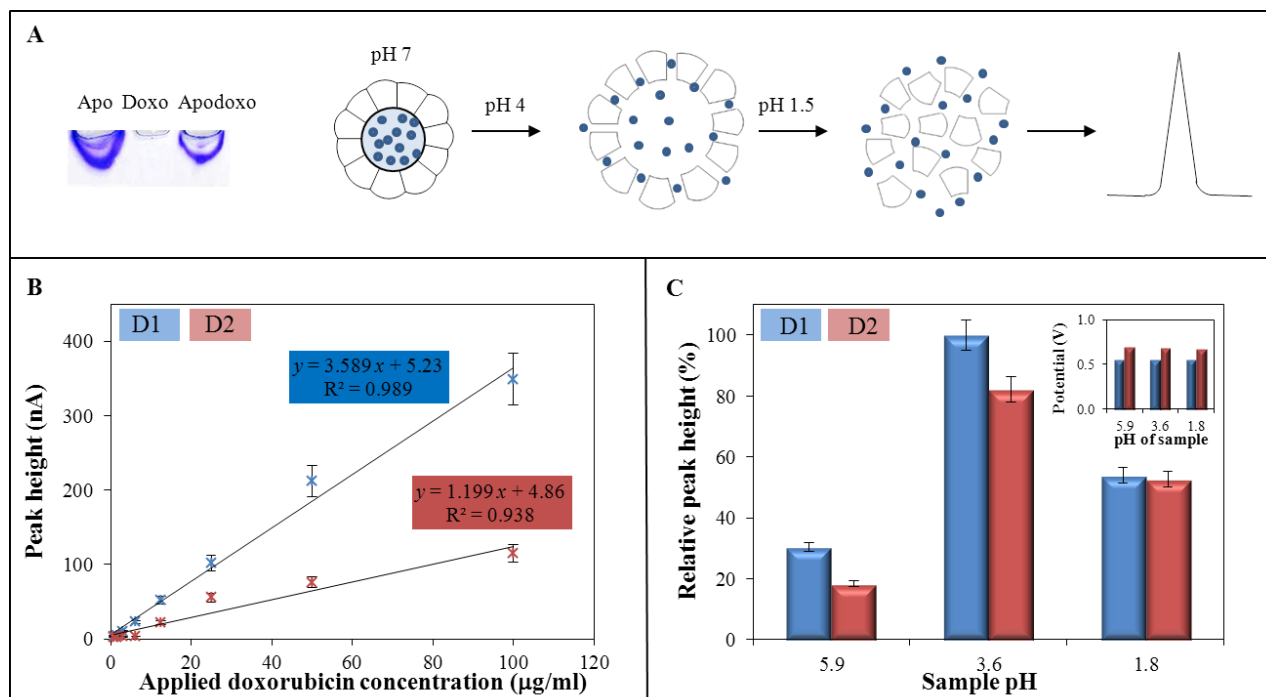


**Figure 3.** (A) Gel electrophoresis of apoferritin (2 mg/ml), doxorubicin (20  $\mu\text{g/ml}$ ) and doxorubicin in apoferritin (2 mg/ml). Scheme of opening apoferritin and 'flowing out' of doxorubicin. (B) Calibration curve of encapsulated doxorubicin (applied concentration) in apoferritin measured in phosphate buffer (pH 5.5), pH of sample 4.0 (1900 + 100 ml). Dependences were measured for two peaks (blue dots – peak around -0.55 V, red dots – around -0.68 V). (C) Dependence of change signal in complex apoferritin-doxorubicin on pH. Dependences were measured for two peaks (blue columns – peak around -0.55 V, red columns – around -0.68 V). Results are obtained for for 25  $\mu\text{g/ml}$  of doxorubicin in apoferritin, (1900 + 100 ml). Inset represents changes of potential on pH. DPV parameters were as follow: Initial potential -1.0 V, end potential 0 V, amplitude 0.05 V, pulse width 0.2 s, pulse period 0.5 s.

An electrochemical approach for detection of individual single nucleotide polymorphisms (SNPs) based on nucleobase-conjugated apoferritin probe loaded with metal phosphate nanoparticles is reported in the following paper [76]. Encapsulating of doxorubicin into apoferritin structure can be done by changing of solution pH (Fig. 3A). Validation of doxorubicin in apoferritin was done by gel



electrophoresis of apoferritin (2 mg/ml), doxorubicin (20 µg/ml) and doxorubicin in apoferritin (2 mg/ml). The gel 6% non-denaturing native PAGE (60 mM glycine, 7 mM acetic acid pH 4) and 50% glycerol like loading buffer were used. Gel runs 90 min at 10 mA. After electrophoresis formed bands were visualized with Coomassie-blue. Band for apoferritin (protein) and apoferritin with doxorubicin are visible compare to single doxorubicin. Value of pH can affect the apoferritin structure and thus form of encapsulated doxorubicin [77].

Formation of complex doxorubicin and apoferritin was made by pH 7 and then the pH was decreased. Decreasing pH (lower than pH 4) caused breakage of apoferritin structure and releasing doxorubicin molecules [78]. The dependence of measured electrochemical signal on applied doxorubicin concentrations, which was used for complex preparation, is shown in Fig. 3B. Each sample was acidified to pH 4.0 (doxorubicin flows to the buffer) and 100 µl of this solution were measured in phosphate buffer pH 5.5 (apoferritin is closed, some doxorubicin molecules remains in the buffer). In doxo and apoferritin mixture, the detected signals of doxorubicin were for about 40% lower compared to corresponding applied concentrations. For D1 peak, the equation was  $y = 3.589x + 5.23$ ,  $R^2 = 0.989$ ,  $n = 4$ , R.S.D. = 44 and for D2 peak  $y = 1.199x + 4.86$ ,  $R^2 = 0.938$ ,  $n = 4$ , R.S.D. = 21.

In addition, change of electrochemical signals from both characteristic peaks (D1 and D2) due to pH change of sample for 25 µg/ml applied doxorubicin concentration was monitored (Fig. 3C). 100 µl of sample was acidified to pH 3.6 and 1.8 and added to 1900 µl of phosphate sample (pH 5.5). In the acid step apoferritin structure is opened, doxorubicin follows out, after transfer to buffer, apoferritin is closed and some molecules of doxorubicin are encapsulated. The residual doxorubicin in solution was detected. In the case of pH 5.9 sample, structure was not opened, thus we detected only doxorubicin after preparation of encapsulated doxorubicin. In inset in Fig. 3C there is showed the shift of potential for D1 and D2 due to pH. The potential range for D1 is between -0.549 to -0.556 and for D2 between -0.695 to -0.676. Thus the potential is not dependent on pH of sample.

### 3.4 Isolation of enclosed doxorubicin in biotinylated apoferritin with magnetic beads

Fig. 4A describes the preparation of isolation procedure of biotinylated apoferritin with encapsulated doxorubicin by magnetic beads. The first step is washing (PBS) of Dynabeads M-270 Streptavidin according to the following protocol. The beads were resuspended and placed to magnetic holder. The supernatant was carefully sucked out and beads were washed. The washing was repeated 3 times. The supernatant was sucked out and 100 µl of sample (biotinylated apoferritin) was added (parts 1+2). Solution was incubated at room temperature on rotator (60 rpm, 90 °C) for 30 min, vibration was turned off. Tube was put to magnetic holder for 2 – 3 min (part 3) and supernatant was poured out. Particles were 3 or 4 times washed with 100 µl PBS (pH 7.4, part 4), after that they were resuspended in 100 µl PBS (pH 7.4). After the sample was acidified and apoferritin structure broken, doxorubicin was released. This effect was measured electrochemically. 100 µl of acid sample were put to the 1900 µl phosphate buffer, pH 5.5.

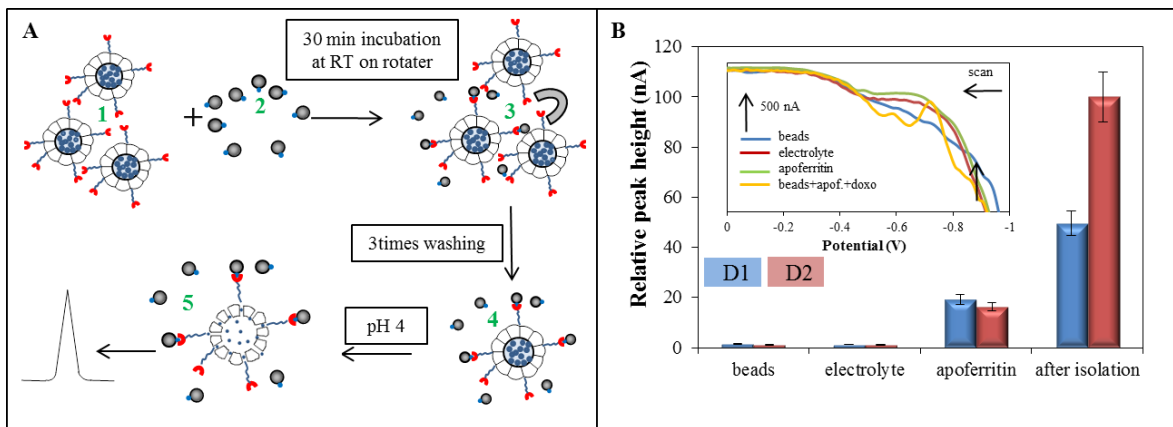


**Figure 4.** Biotinylated apoferritin with doxorubicin and streptavidin magnetic beads. (A) Scheme of interaction biotinylated apoferritin with doxorubicin and streptavidin magnetic beads. 1 - doxorubicin in the biotinylated apoferritin (red part is biotinyl), 2 - streptavidin magnetic beads (blue part is streptavidin), 3 - solution consists of biotinylated apoferritin and magnetic beads, 4 - binding biotinylated apoferritin to magnetic parts (biotin – streptavidin binding), 5 – opening of binding biotinylated apoferritin with streptavidin magnetic parts. (B) Relative peak height of magnetic beads, electrolyte, apoferritin and biotinylated apoferritin with doxorubicin and streptavidin magnetic beads, concentration of encapsulated doxorubicin (applied concentration) is 100 µg/ml, pH of sample 6.3. Insert shows voltammograms for different components. DPV parameters were as it follows: initial potential -1.0 V, end potential 0 V, amplitude 0.05 V, pulse width 0.2 s, pulse period 0.5 s, deposition potential -1.0 V and time of accumulation 120 s. Phosphate buffer (0.1 M, pH 5.5) was used as a supporting electrolyte.

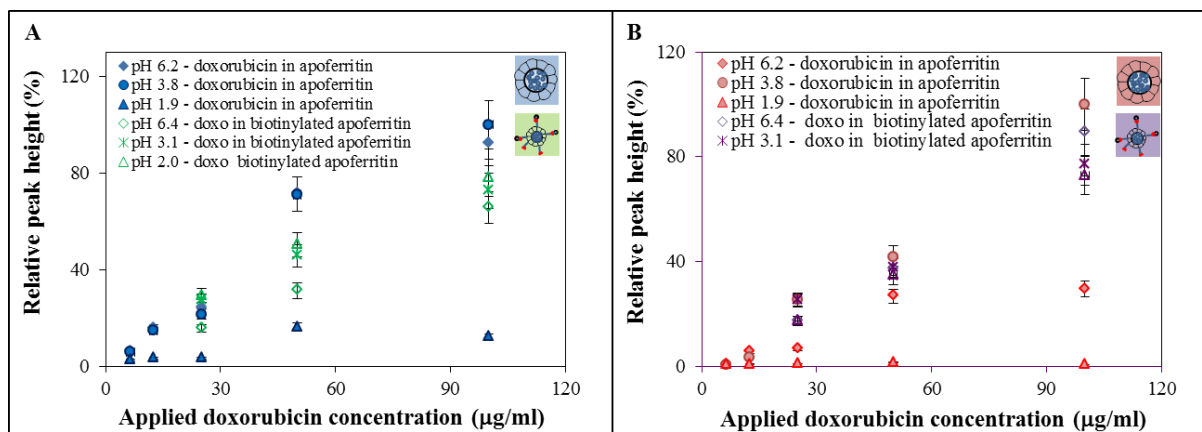


**Figure 5.** Changes of electrochemical signals of encapsulated doxorubicin (applied concentration) in apoferritin due to samples pH. Doxorubicin voltammogram with two characteristic peaks at -0.55 V (blue/green) and -0.68 V (red/violet), doxo concentration 100 µg/ml. (A) Different doxorubicin concentrations encapsulated in apoferritin (blue)/in biotinylated apoferritin (green) and flowing out of doxorubicin due to pH changes. (B) Different doxorubicin concentrations encapsulated in apoferritin (red)/in biotinylated apoferritin (violet) and flowing out of doxorubicin due to pH changes. All experiments were measured by DPV at carbon paste.

Measured data are indicated in Fig. 4B. It is clear that magnetic beads and electrolyte did not give any peak in the position of the interest (at -0.55 V and -0.68 V). Single apoferritin had some peaks, but signals were low (for D1 approximately 30% according to biotinylated apoferritin with doxo, for D2 only 19% of signal according to tested sample) and the position of these peaks were shifted (-0.46 V and -0.53 V). Inserted picture shows voltammogram for beads, apoferritin and apoferritin with doxorubicin with typical two peaks.

The comparison of recovery ratios of doxorubicin encapsulated/opened in apoferritin to doxorubicin encapsulated/opened in biotinylated apoferritin with magnetic beads is shown in Fig. 5A (D1 peak) and in Fig. 5B (D2 peak). The amount of doxorubicin after isolation, i.e. biotinylated doxorubicin with magnetic beads, is lower than before isolation. The highest value for pH 3.8 apoferritin in doxorubicin (100 µg/ml) was obtained for D1 peak. D1 peak under the same conditions for biotinylated apoferritin with doxorubicin had only 73 % of this value. There is not big difference for biotinylated apoferritin with doxorubicin for signal at different pH (D1-12 %, D2-15 %). Dramatic decreasing is in the signal among apoferritin with doxo at pH 3.8 and pH 1.9 for both peaks. pH 6.2 has lowest value from all three pHs. Showed curve has similar progress such it was demonstrated in Fig. 3C.

#### 4. CONCLUSIONS

Cytostatics have great toxic effect on cells [79]. Due to this numerous groups are focused on discovering nanovehicles for transporting of cytostatic to the right place with minimization of the side effects. In this article it is shown functional nanovehicle - apoferritin, where doxorubicin can be encapsulated and the influence of pH is studied. It was shown that pH decreasing lower than 4 was sufficient for the opening of apoferritin structure and doxorubicin can flow out and affects the illness species.

#### ACKNOWLEDGEMENTS

Financial support from CEITEC CZ.1.05/1.1.00/02.0068, LPR 2012/2013 and CYTORES GA CR P301/10/0356 is highly acknowledged. The authors wish to thank to Jiri Kudr for perfect technical assistance.

#### References

1. G. Minotti, P. Menna, E. Salvatorelli, G. Cairo and L. Gianni, *Pharm. Rev.*, 56 (2004) 185.
2. M. Stiborova, T. Eckschlager, J. Poljakova, J. Hrabeta, V. Adam, R. Kizek and E. Frei, *Curr. Med. Chem.*, 19 (2012) 4218.

3. M. Stiborova, J. Poljakova, T. Eckschlager, R. Kizek and E. Frei, *Biomed. Pap-Olomouc*, 156 (2012) 115.
4. D. Hynek, L. Krejcova, O. Zitka, V. Adam, L. Trnkova, J. Sochor, M. Stiborova, T. Eckschlager, J. Hubalek and R. Kizek, *Int. J. Electrochem. Sci.*, 7 (2012) 13.
5. D. Hynek, L. Krejcova, O. Zitka, V. Adam, L. Trnkova, J. Sochor, M. Stiborova, T. Eckschlager, J. Hubalek and R. Kizek, *Int. J. Electrochem. Sci.*, 7 (2012) 34.
6. R. Kizek, V. Adam, J. Hrabeta, T. Eckschlager, S. Smutny, J. V. Burda, E. Frei and M. Stiborova, *Pharmacol. Ther.*, 133 (2012) 26.
7. S. Zhang, X. B. Liu, T. Bawa-Khalife, L. S. Lu, Y. L. Lyu, L. F. Liu and E. T. H. Yeh, *Nat. Med.*, 18 (2012) 1639.
8. Y. Bernard, N. Ribeiro, F. Thuaud, G. Turkeri, R. Dirr, M. Boulberdaa, C. G. Nebigil and L. Desaubry, *PLoS One*, 6 (2011) 1.
9. J. Y. Hwang, J. Park, B. J. Kang, D. J. Lubow, D. Chu, D. L. Farkas, K. K. Shung and L. K. Medina-Kauwe, *PLoS One*, 7 (2012) 1.
10. V. K. Todorova, M. L. Beggs, R. R. Delongchamp, I. Dhakal, I. Makhoul, J. Y. Wei and V. S. Klimberg, *PLoS One*, 7 (2012) 1.
11. H. G. Keizer, H. M. Pinedo, G. J. Schuurhuis and H. Joenje, *Pharmacol. Ther.*, 47 (1990) 219.
12. R. R. Patil, S. A. Guhagarkar and P. V. Devarajan, *Crit. Rev. Ther. Drug Carr. Syst.*, 25 (2008) 1.
13. A. Schroeder, D. A. Heller, M. M. Winslow, J. E. Dahlman, G. W. Pratt, R. Langer, T. Jacks and D. G. Anderson, *Nat. Rev. Cancer*, 12 (2012) 39.
14. M. Ryvolova, V. Adam, T. Eckschlager, M. Stiborova and R. Kizek, *Electrophoresis*, 33 (2012) 1545.
15. D. Agudelo, P. Bourassa, J. Bruneau, G. Berube, E. Asselin and H. A. Tajmir-Riahi, *PLoS One*, 7 (2012) 1.
16. M. L. Huan, B. Zhang, Z. H. Teng, H. Cui, J. P. Wang, X. Y. Liu, H. Xia, S. Y. Zhou and Q. B. Mei, *PLoS One*, 7 (2012) 1.
17. J. Lin, Y. Yu, S. Shigdar, D. Z. Fang, J. R. Du, M. Q. Wei, A. Danks, K. Liu and W. Duan, *PLoS One*, 7 (2012) 1.
18. H. Li and Z. H. Qian, *Med. Res. Rev.*, 22 (2002) 225.
19. A. E. H. de Mendoza, M. A. Campanero, F. Mollinedo and M. J. Blanco-Prieto, *J. Biomed. Nanotechnol.*, 5 (2009) 323.
20. S. Jaracz, J. Chen, L. V. Kuznetsova and L. Ojima, *Bioorg. Med. Chem.*, 13 (2005) 5043.
21. R. Xing, X. Wang, C. Zhang, Y. Zhang, Q. Wang, Z. Yang and Z. Guo, *J. Inorg. Biochem.*, 103 (2009) 1039.
22. S. T. Yau and P. G. Vekilov, *Nature*, 406 (2000) 494.
23. S. Granick, *Science*, 103 (1946) 107.
24. M. Uchida, M. T. Klem, M. Allen, P. Suci, M. Flenniken, E. Gillitzer, Z. Varpness, L. O. Liepold, M. Young and T. Douglas, *Adv. Mater.*, 19 (2007) 1025.
25. C. Salis, C. J. Goedelmann, J. M. Pasquini, E. F. Soto and C. P. Setton-Avruj, *Dev. Neurosci.*, 24 (2002) 214.
26. M. S. Bretscher and J. N. Thomson, *Embo J.*, 2 (1983) 599.
27. R. L. Fan, S. W. Chew, V. V. Cheong and B. P. Orner, *Small*, 6 (2010) 1483.
28. M. A. Kilic, E. Ozlu and S. Calis, *J. Biomed. Nanotechnol.*, 8 (2012) 508.
29. E. Simsek and M. A. Kilic, *Journal of Magnetism and Magnetic Materials*, 293 (2005) 509.
30. F. Patolsky, E. Katz and I. Willner, *Angew. Chem.-Int. Edit.*, 41 (2002) 3398.
31. H. Berg, G. Horn, H. E. Jacob, U. Fiedler, U. Luthardt and D. Tresselt, *Bioelectrochem. Bioenerg.*, 16 (1986) 135.

32. J. Wang, M. S. Lin and V. Villa, *Analyst*, 112 (1987) 1303.
33. J. B. Hu, Q. Q. Huang and Q. L. Li, *Chin. Sci. Bull.*, 46 (2001) 1355.
34. K. Hashimoto, K. Ito and Y. Ishimori, *Anal. Chim. Acta*, 286 (1994) 219.
35. D. Abd El-Hady, M. I. Abdel-Hamid, M. M. Seliem and N. A. El-Maali, *Talanta*, 66 (2005) 1207.
36. D. Huska, V. Adam, J. Hubalek, L. Trnkova, T. Eckschlager, M. Stiborova, I. Provaznik and R. Kizek, *Chim. Oggi-Chem. Today*, 28 (2010) 18.
37. D. Huska, V. Adam, S. Krizkova, J. Hrabeta, T. Eckschlager, M. Stiborova and R. Kizek, *Chim. Oggi-Chem. Today*, 28 (2010) 15.
38. S. Eynollahi, S. Riahi, M. R. Ganjali and P. Norouzi, *Int. J. Electrochem. Sci.*, 5 (2010) 1367.
39. T. R. R. Naik and H. S. B. Naik, *Int. J. Electrochem. Sci.*, 3 (2008) 409.
40. S. Riahi, S. Eynollahi, M. R. Ganjali and P. Norouzi, *Int. J. Electrochem. Sci.*, 5 (2010) 1151.
41. S. Riahi, S. Eynollahi, M. R. Ganjali and P. Norouzi, *Int. J. Electrochem. Sci.*, 5 (2010) 815.
42. S. Riahi, S. Eynollahi, M. R. Ganjali and P. Norouzi, *Int. J. Electrochem. Sci.*, 5 (2010) 355.
43. M. Masarik, L. Krejcova, D. Hynek, V. Adam, M. Stiborova, T. Eckschlager and R. Kizek, *Int. J. Mol. Med.*, 30 (2012) S45.
44. D. Huska, V. Adam, J. Burda, J. Hrabeta, T. Eckschlager, P. Babula, R. Opatrilova, L. Trnkova, M. Stiborova and R. Kizek, *FEBS. J.*, 276 (2009) 109.
45. M. Masarik, H. Kynclova, D. Huska, J. Hubalek, V. Adam, P. Babula, T. Eckschlager, M. Stiborova and R. Kizek, *Int. J. Mol. Med.*, 26 (2010) S46.
46. D. Huska, V. Adam, P. Babula, J. Hrabeta, M. Stiborova, T. Eckschlager, L. Trnkova and R. Kizek, *Electroanalysis*, 21 (2009) 487.
47. M. Masarik, D. Huska, V. Adam, J. V. Burda, T. Eckschlager, M. Stiborova and R. Kizek, *Int. J. Mol. Med.*, 24 (2009) S49.
48. R. Prusa, D. Huska, V. Adam, J. Kukacka, J. Hrabeta, T. Eckschlager, P. Babula, M. Stiborova, L. Trnkova and R. Kizek, *Clin. Chem.*, 55 (2009) A217.
49. L. Trnkova, M. Stiborova, D. Huska, V. Adam, R. Kizek, J. Hubalek and T. Eckschlager, Electrochemical biosensor for investigation of anticancer drugs interactions (doxorubicin and ellipticine) with DNA, 2009.
50. Y. H. Hahn and H. Y. Lee, *Arch. Pharm. Res.*, 27 (2004) 31.
51. D. Abd El-Hady, M. I. Abdel-Hamid, M. M. Seliem and N. A. E-Maali, *Arch. Pharm. Res.*, 27 (2004) 1161.
52. S. M. Golabi and D. Nematollahi, *J. Pharm. Biomed. Anal.*, 10 (1992) 1053.
53. H. M. Zhang and N. Q. Li, *J. Pharm. Biomed. Anal.*, 22 (2000) 67.
54. S. Zhang, K. Wu and S. Hu, *Anal. Sci.*, 18 (2002) 1089.
55. I. N. Rodriguez, J. A. M. Leyva and J. L. H. H. deCisneros, *Anal. Chim. Acta*, 344 (1997) 167.
56. S. Komorsky-Lovric and M. Lovric, *Collect. Czech. Chem. Commun.*, 72 (2007) 1398.
57. Y. Z. Fang, S. H. Liu and P. G. He, *Chem. J. Chin. Univ.-Chin.*, 17 (1996) 1222.
58. S. Komorsky-Lovric, *Bioelectrochemistry*, 69 (2006) 82.
59. Z. Jemelkova, J. Zima and J. Barek, *Collect. Czech. Chem. Commun.*, 74 (2009) 1503.
60. M. S. Ibrahim, Z. A. Ahmed, Y. M. Temerk and H. Berg, *Bioelectrochem. Bioenerg.*, 36 (1995) 149.
61. H. Ali-Boucetta, K. T. Al-Jamal and K. Kostarelos, Multi-Walled Carbon Nanotube-Doxorubicin Supramolecular Complexes for Cancer Therapeutics, CRC Press-Taylor & Francis Group, Boca Raton, 2008.
62. J. Prasek, J. Drbohlavova, J. Chomoucka, J. Hubalek, O. Jasek, V. Adam and R. Kizek, *J. Mater. Chem.*, 21 (2011) 15872.
63. H. Jiang and X. M. Wang, *Electrochem. Commun.*, 11 (2009) 126.

64. D. Dospivova, D. Hynek, P. Kopel, A. Bezdekova, J. Sochor, S. Krizkova, V. Adam, L. Trnkova, J. Hubalek, P. Babula, I. Provaznik, R. Vrba and R. Kizek, *Int. J. Electrochem. Sci.*, 7 (2012) 6378.
65. Z. R. Ying, X. M. Lin, Y. Qi and J. Luo, *Mater. Res. Bull.*, 43 (2008) 2677.
66. G. L. Long and J. D. Winefordner, *Anal. Chem.*, 55 (1983) A712.
67. I. Svancara and J. Zima, *Curr. Org. Chem.*, 15 (2011) 3043.
68. J. Hubalek, J. Prasek, D. Huska, M. Adamek, O. Jasek, V. Adam, L. Trnkova, A. Horna and R. Kizek, in J. Brugger, D. Briand (Editors), Proceedings of the Eurosensors XXIII Conference, 2009, p. 1011.
69. R. Kizek, M. Masarik, K. J. Kramer, D. Potesil, M. Bailey, J. A. Howard, B. Klejdus, R. Mikelova, V. Adam, L. Trnkova and F. Jelen, *Anal. Bioanal. Chem.*, 381 (2005) 1167.
70. S. Krizkova, V. Hrdinova, V. Adam, E. P. J. Burgess, K. J. Kramer, M. Masarik and R. Kizek, *Chromatographia*, 67 (2008) S75.
71. J. Petrlava, S. Krizkova, V. Supalkova, M. Masarik, V. Adam, L. Havel, K. J. Kramer and R. Kizek, *Plant Soil Environ.*, 53 (2007) 345.
72. J. Prasek, J. Hubalek, M. Adamek and R. Kizek, in 2006 IEEE Sensors, Vols 1-3, 2006, p. 1261.
73. V. Shestivska, V. Adam, J. Prasek, T. Macek, M. Mackova, L. Havel, V. Diopan, J. Zehnalek, J. Hubalek and R. Kizek, *Int. J. Electrochem. Sci.*, 6 (2011) 2869.
74. D. Dospivova, K. Smerkova, M. Ryvolova, D. Hynek, V. Adam, P. Kopel, M. Stiborova, T. Eckschlager, J. Hubalek and R. Kizek, *Int. J. Electrochem. Sci.*, 7 (2012) 3072.
75. P. Yousefpour, F. Atyabi, E. V. Farahani, R. Sakhtianchi and R. Dinarvand, *Int. J. Nanomed.*, 6 (2011) 1487.
76. A. Abbaspour and A. Noori, *Biosens. Bioelectron.*, 37 (2012) 11.
77. G. D. Liu, J. Wang, H. Wu, Y. Y. Lin and Y. H. Lin, *Electroanalysis*, 19 (2007) 777.
78. M. Kim, Y. Rho, K. S. Jin, B. Ahn, S. Jung, H. Kim and M. Ree, *Biomacromolecules*, 12 (2011) 1629.
79. S. Krizkova, M. Ryvolova, J. Hrabeta, V. Adam, M. Stiborova, T. Eckschlager and R. Kizek, *Drug Metab. Rev.*, 44 (2012) 287.